

Supporting information

Self-assembly amphiphilic polysaccharide-based co-delivery system for egg white derived peptides and curcumin with oral bioavailability enhancement

Meng Yang,^a Jingbo Liu,^a Yajuan Li,^a Qi Yang,^a Xuanting Liu,^a Chunmei Liu,^a Sitong Ma,^a
Boqun Liu,^a Ting Zhang,^a Hang Xiao^b and Zhiyang Du^{a,*}

^a Jilin Provincial Key Laboratory of Nutrition and Functional Food, College of Food Science
and Engineering, Jilin University, Changchun 130062, China

^b Department of Food Science, University of Massachusetts, Amherst, Massachusetts 01003,
USA

* Corresponding author, E-mail: dzy2635@163.com

Phone number: +86 18686407106

16 **Methods**

17 **Transmission Electron Microscopy (TEM).** TEM images were conducted with a Tecnai
18 Spirit electron microscope (FEI, Netherlands). Each of sample solution was dropped onto a
19 copper wire mesh and negatively stained by phosphotungstic acid in advance¹.

20 **Atomic Force Microscopy (AFM).** The AFM observation for samples was performed
21 using a Veeco Nanoscope V Multimode 8 scanning probe microscope under the ambient
22 conditions (25 °C, relative humidity of 25%). Prior to AFM scanning, 10 µL of each sample
23 was dropped on the smooth mica sheets carefully and air-dried for 4 h.

24 **X-ray Photoelectron Spectroscopy (XPS).** The surface elemental composition of
25 samples was detected by a Thermo ESCALAB 250Xi spectrometer (Waltham, MA) using an
26 Al K α X-ray excitation source. The high-resolution spectra were obtained at a 30.00 eV pass
27 energy with a step size of 0.050 eV².

28 **Fourier Transform Infrared Spectroscopy (FTIR).** FTIR was performed to explore the
29 interaction mechanism within the NPs. Different samples were freeze-dried in advance and
30 then made into tablets at a specific mass ratio (sample:potassium bromide = 1:100). The
31 corresponding spectra were recorded at a resolution of 4 cm⁻¹ over the 4000-400 cm⁻¹ range.

32 **¹H NMR.** Lyophilized samples were fully dissolved in deuterated dimethyl sulfoxide
33 (DMSO-d₆) to reach a concentration of 5 mg/mL. Then, the ¹H NMR spectra was determined
34 by a Bruker Advance III 500 MHz spectrometer (Billerica, MA). The chemical shifts were
35 reported in ppm, respectively³.

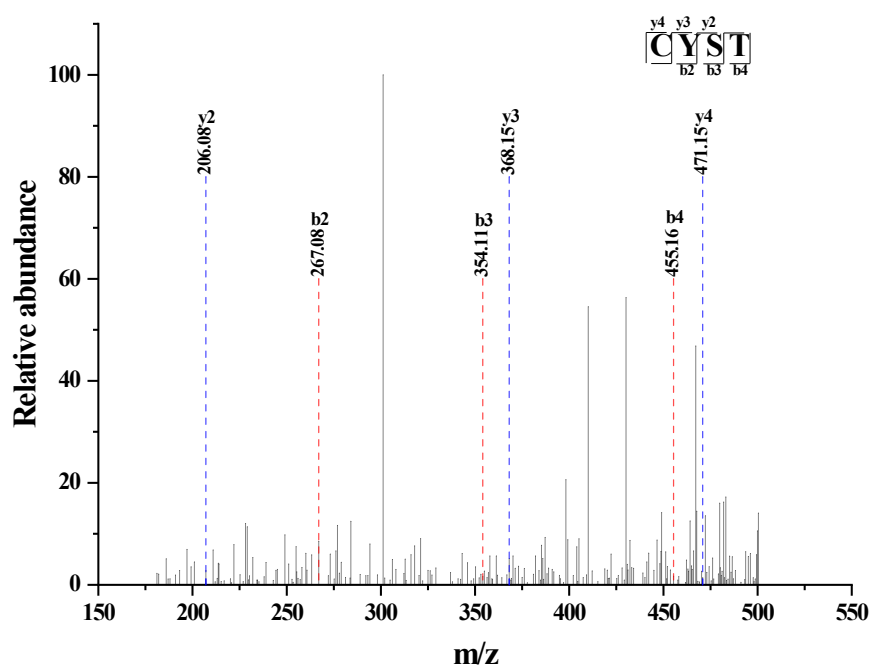
36 **X-ray Diffraction (XRD).** To better illustrate the co-encapsulation mechanism of EWDP
37 and curcumin in NPs, freeze-dried samples were detected by an X-ray diffractometer (Bruker,
38 Germany) with 40 kV accelerating voltage and 40 mA tube current. The 2 θ angel range was
39 set as 5-50° with a scanning rate of 0.24°/min⁴.

40 **Differential Scanning Calorimetry (DSC).** DSC was performed to investigate the
41 thermal properties and crystallinity of NPs. Samples were heated from 30 to 230 °C (10 °C/min)
42 in the hermetically sealed aluminum pans with a nitrogen flow of 20 mL/min⁵.

43 **Cytotoxicity Assay** Caco-2 cells were grown in Dulbecco's modified Eagle's medium
44 (DMEM) containing 10% fetal bovine serum, 1% nonessential amino acid and 1% penicillin-

45 streptomycin. The cells (90 μ L) were seeded in the 96-well plates with a density of 8000 cells
46 per well, respectively. After overnight incubation, the cells were exposed to the samples (10
47 μ L) diluted in phosphate buffered saline (PBS) with different EWDP/curcumin concentrations
48 for 24 h. Afterwards, 20 μ L MTS solution was loaded to each well for 2 h (37 $^{\circ}$ C, 5% CO₂),
49 and then the UV absorbance at 490 nm was recorded by a microplate reader (BioTek,
50 Winooski, VT) to calculate the corresponding cell viability⁶.

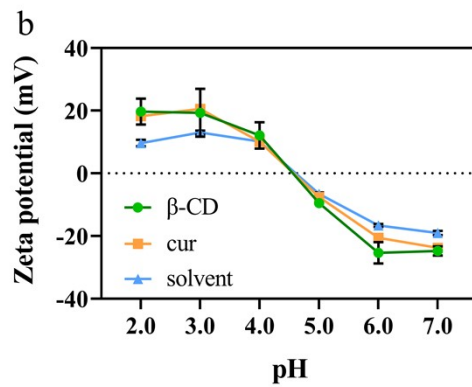
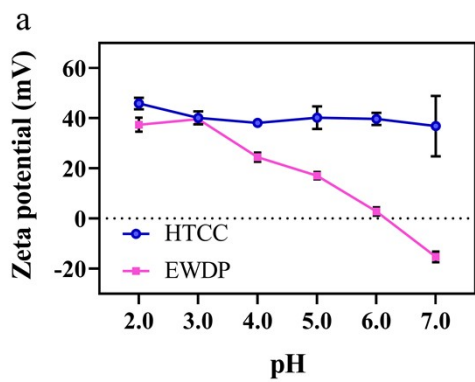
51



53

54 **Fig. S1** The mass spectrum of EWDP (CYST). The corresponding b and y ions were shown
55 in the spectrum.

56



57

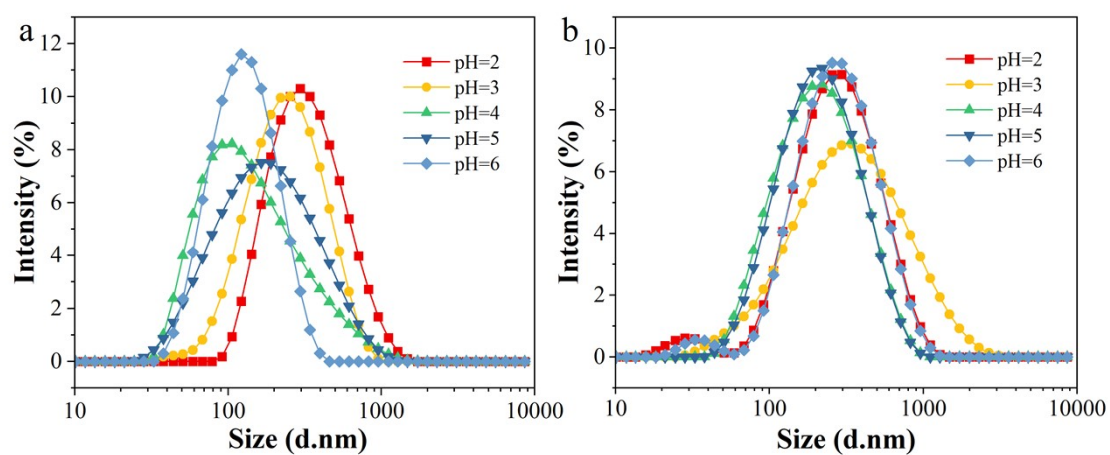
58 **Fig. S2** Zeta potential of native core-shell materials and solvent under various pH values (2.0-

59

7.0).

60

61



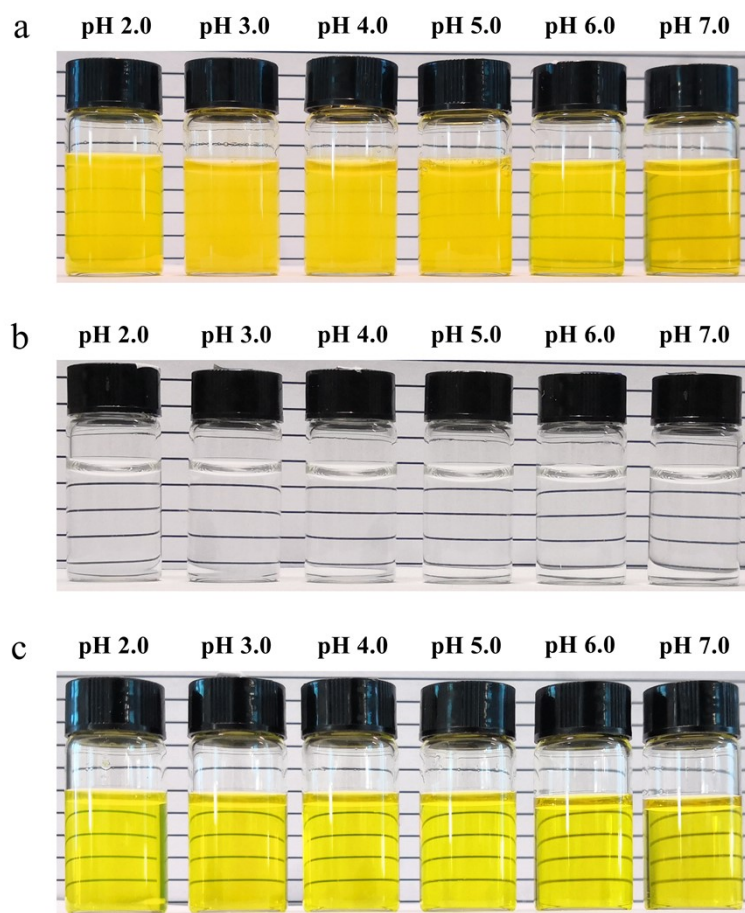
62

63 **Fig. S3** The size distribution of samples under different pH values (2.0-6.0). (a) HTCC-β-CD

64

NPs. (b) HTCC-EWDP-β-CD-cur NPs.

65



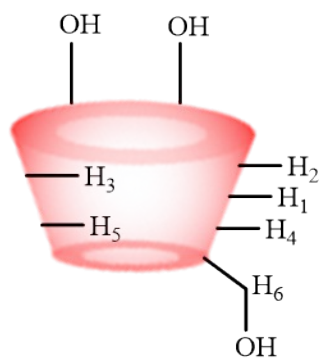
66

67 **Fig. S4** Images of samples under different pH values (2.0-7.0). (a) The simple mixture of

68 EWDP and curcumin. (b) HTCC-β-CD NPs. (c) HTCC-EWDP-β-CD-cur NPs. The

69 concentration of EWDP and curcumin for different samples was 0.5 mg/mL and 0.05 mg/mL.

70



71

72 **Fig. S5** Schematic illustration of different protons distribution within the β-CD molecule.

73

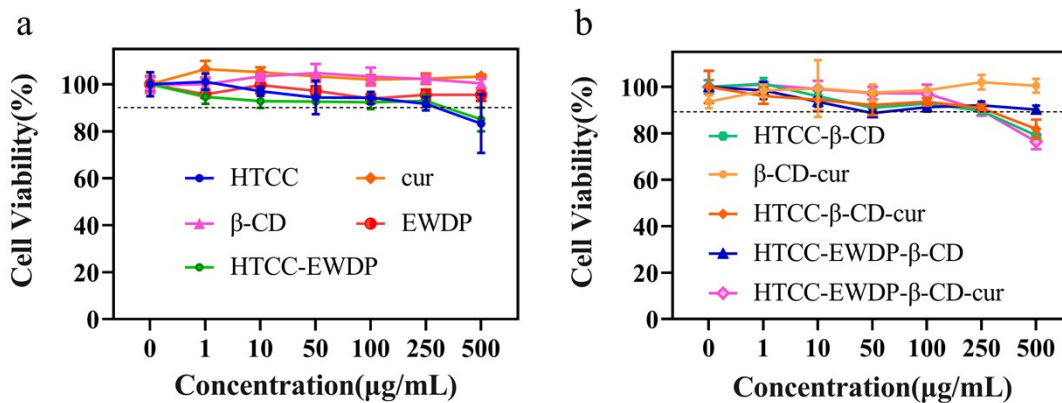
74 **Table S1** ¹H NMR analysis of β-CD protons' chemical shifts within the composite NPs after
 75 encapsulation

Protons	$\Delta\delta_{\text{HTCC-}\beta\text{-CD}}$	$\Delta\delta_{\beta\text{-CD-cur}}$	$\Delta\delta_{\text{HTCC-}\beta\text{-CD-cur}}$	$\Delta\delta_{\text{HTCC-EWDP-}\beta\text{-CD-cur}}$
H1	-0.001	-0.003	-0.004	-0.020
H2	-0.001	-0.004	-0.004	-0.021
H3	0.000	-0.009	-0.009	-0.314
H4	0.003	0.000	-0.001	-0.002
H5	0.000	-0.006	-0.007	-0.024
H6	0.002	-0.005	-0.007	-0.020

76 $\Delta\delta = \delta_{\text{the corresponding NPs}} - \delta_{\beta\text{-CD}}$.

77

78



79

80 **Fig. S6** Cytotoxicity evaluation for different samples. All the samples showed no significant
 81 cytotoxicity on Caco-2 cell after incubation for 24 h (cell viability \geq 90%).

82

83 References

- 84 1 M. Ma, T. Sun, P. Xing, Z. Li, S. Li, J. Su, X. Chu and A. Hao, A supramolecular curcumin vesicle and its
85 application in controlling curcumin release, *Colloids and Surfaces A: Physicochemical and Engineering*
86 *Aspects*, 2014, **459**, 157-165.
- 87 2 X. Hu, Y. Wang, L. Zhang and M. Xu, Construction of self-assembled polyelectrolyte complex hydrogel
88 based on oppositely charged polysaccharides for sustained delivery of green tea polyphenols, *Food*
89 *Chem.*, 2020, **306**, 125632.
- 90 3 S. Goswami and M. Sarkar, Fluorescence, FTIR and ¹H NMR studies of the inclusion complexes of the
91 painkiller lornoxicam with β -, γ -cyclodextrins and their hydroxy propyl derivatives in aqueous solutions
92 at different pHs and in the solid state, *New J. Chem.*, 2018, **42**, 15146-15156.
- 93 4 S. Feng, Y. Sun, D. Wang, P. Sun and P. Shao, Effect of adjusting pH and chondroitin sulfate on the
94 formation of curcumin-zein nanoparticles: Synthesis, characterization and morphology, *Carbohydr.*
95 *Polym.*, 2020, **250**, 116970.
- 96 5 Y. Ren, L. Huang, Y. Wang, L. Mei, R. Fan, M. He, C. Wang, A. Tong, H. Chen and G. Guo,
97 Stereocomplexed electrospun nanofibers containing poly (lactic acid) modified quaternized chitosan for
98 wound healing, *Carbohydr. Polym.*, 2020, **247**, 116754.
- 99 6 J. Xiao, S. Nian and Q. Huang, Assembly of kafirin/carboxymethyl chitosan nanoparticles to enhance the
100 cellular uptake of curcumin, *Food Hydrocolloids*, 2015, **51**, 166-175.

101